

This is an ACCEPTED VERSION of the following published document:

Fresnedo, O., Vazquez-Araujo, F. J., Castedo, L., and Garcia-Frias, J. (2016) Analogue joint source-channel coding for multiple input multiple output–orthogonal frequency division multiplexing systems. *Trans. Emerging Tel. Tech.*, 27: 408–419. doi: [10.1002/ett.2908](https://doi.org/10.1002/ett.2908).

Link to published version: <https://doi.org/10.1002/ett.2908>

General rights:

This is the peer reviewed version of the following article: Fresnedo, O., Vazquez-Araujo, F. J., Castedo, L., and Garcia-Frias, J. (2016) 'Analogue joint source-channel coding for multiple input multiple output–orthogonal frequency division multiplexing systems'. *Trans. Emerging Tel. Tech.*, 27: 408–419, which has been published in final form at <https://doi.org/10.1002/ett.2908>. This article may be used for non-commercial purposes in accordance with [Wiley Terms and Conditions for Use of Self-Archived Versions](#). This article may not be enhanced, enriched or otherwise transformed into a derivative work, without express permission from Wiley or by statutory rights under applicable legislation. Copyright notices must not be removed, obscured or modified. The article must be linked to Wiley's version of record on Wiley Online Library and any embedding, framing or otherwise making available the article or pages thereof by third parties from platforms, services and websites other than Wiley Online Library must be prohibited.

Analog Joint Source-Channel Coding for MIMO-OFDM Systems

O. Fresnedo^{1*}, F. J. Vazquez-Araujo¹, L. Castedo¹ and J. Garcia-Frias²

¹Department of Electronics and Systems, University of A Coruña, Spain.

²Department of Electrical and Computer Engineering, University of Delaware, USA.

ABSTRACT

Analog Joint Source-Channel Coding (JSCC) has been shown to approach the optimal distortion-cost trade-off when transmitting over AWGN channels. In this work we consider analog JSCC over frequency-selective channels using Orthogonal Frequency Division Multiplexing (OFDM) modulation and multiple antennas at transmission and/or reception, i.e. using a MIMO-OFDM system. Due to its high complexity, optimal MMSE analog JSCC decoding is infeasible in MIMO-OFDM systems and a practical two-stage decoding approach made up of an MMSE estimator followed by a Maximum Likelihood (ML) decoder is proposed instead. Three different alternatives for system optimization are considered: non-adaptive coding, adaptive coding, and adaptive coding with precoding. We show that the three considered strategies approach the optimal distortion-cost trade-off, but the best performance is obtained with the adaptive coding scheme when precoding is utilized. Copyright © 0000 John Wiley & Sons, Ltd.

*Correspondence

E-mail: oscar.fresnedo@udc.es. Facultad de Informática, Campus Elviña s/n, 15071, A Coruña.

1. INTRODUCTION

Source compression and channel coding are typically performed separately in most digital communication systems. This communication strategy, known as the “separation principle”, has been shown to be optimum for both lossless compression [1] and lossy compression [2] of analog sources. However, when digital communication systems are designed to perform close to the optimal distortion-cost trade-off, sources have to be compressed using powerful Vector Quantization (VQ) and entropy coding methods, and data has to be transmitted utilizing capacity approaching digital codes that use long block lengths and introduce significant delay and high computational complexity. Moreover, full redesign of the digital system is required whenever

a change is required in either the data rate or the distortion target.

Recently, discrete-time analog communication systems based on the transmission of continuous amplitude channel symbols have been proposed as an alternative to digital communication systems. As shown in [3–5], using appropriate analog Joint Source Channel Coding (JSCC) techniques, it is possible to approach the optimal distortion-cost trade-off at high data rates with very low complexity and an almost negligible delay. In addition, analog JSCC schemes are more robust than standard digital systems to changes in the channel conditions, and they can be continuously adapted to the channel fluctuations on time-varying environments by updating the encoder parameters at the transmitter. These appealing properties make

analog JSCC strategies specially suitable for high-speed transmissions with severe constraints on delay and/or power consumption over fading channels such as real-time communications over wireless channels or sensor networks [6].

Most previous work in analog JSCC focuses on AWGN channels, while analog JSCC over wireless channels has deserved less attention in the literature. As an example, references [7, 8] consider the use of spatial diversity to improve the performance of analog JSCC in wireless fading channels. Another example is [9], where the transmission of analog samples over single-carrier Multiple Input Multiple Output (MIMO) fading channels is considered. It is also worth mentioning reference [10] where the implementation on a Software Defined Radio testbed of a wireless system based on analog JSCC is presented. Excellent performance over wireless channels is attained when the encoder parameters are continuously adapted to the time-varying Channel Signal to Noise Ratio (CSNR).

In this work we consider analog JSCC over frequency-selective channels using Orthogonal Frequency Division Multiplexing (OFDM) modulation. When combined with MIMO transmission over multiple transmit and receive antennas, the resulting signaling method is referred to as MIMO-OFDM. This transmission method has been adopted by the last generation of broadband wireless communication systems due to its ability to achieve large spectral efficiencies while enabling low-complexity equalization of frequency-selective channels.

This work goes several steps further than that presented in [9]. On the one hand, it considers the more realistic case of broadband frequency-selective MIMO channels and extends the design of analog JSCC narrowband frequency-flat MIMO systems proposed in [9] to also include the transmission of OFDM symbols. Notice that complexity of broadband MIMO-OFDM systems is significantly larger than that of narrowband single-carrier MIMO ones and this largely impacts on system optimization. On the other hand, it considers transmission strategies not addressed in [9] and discusses their optimization. More specifically, three different strategies are considered depending on

the level of channel knowledge at the transmitter: non-adaptive coding, adaptive coding, and adaptive coding with linear precoding. We show that significant performance gains are obtained when linear precoding is designed according to the MMSE criterion [11–13] and utilized to exploit the Channel State Information (CSI) at transmission. Related to system optimization, special attention is paid to the normalization operation required at the encoder output. In particular, the utilization of OFDM symbols allows for either using the time or the frequency dimension to normalize the analog JSCC symbols.

This paper is organized as follows. Section 2 reviews the basics of analog JSCC systems. Section 3 focuses on the specifics of analog JSCC in MIMO-OFDM systems. Section 4 explores the adaptation of the analog encoder parameters to the channel characteristics in order to improve system performance. Section 5 presents the results of computer experiments and Section 6 is devoted to the conclusions.

2. ANALOG JOINT SOURCE-CHANNEL CODING

Figure 1 shows the block diagram of a discrete-time $N:1$ bandwidth compression analog JSCC communication system. At the transmitter, N independent and identically-distributed (i.i.d.) source symbols are grouped into the source vector $\mathbf{x} = [x_1, x_2, \dots, x_N]^T$ and compressed into one channel symbol s . The superindex T denotes transposition. The analog encoding consists of three steps: compression, $M_\delta(\cdot)$; non-linear transformation, $T_\alpha(\cdot)$; and normalization, $1/\sqrt{\gamma}$.

Recent work on analog JSCC [3–5, 14] proposes the use of Shannon-Kotel'nikov mappings to define the compression functions $M_\delta(\cdot)$ that map the N -dimensional source vector \mathbf{x} into a single value $\hat{\theta}$. In the particular case of $N = 2$, Akyol et al. [15] have shown that the optimal 2:1 mapping quite resembles a spiral-like space-filling curve. For that reason, we specifically consider the Archimedes' spiral whose

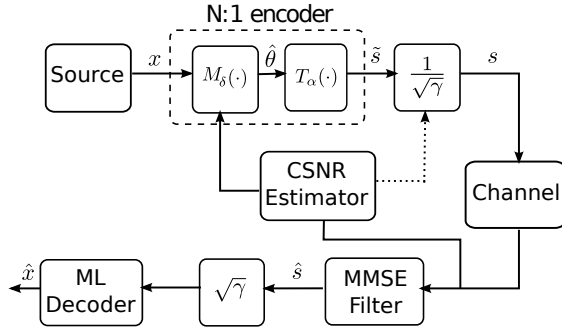


Figure 1. Block diagram of an analog JSCC system.

mathematical expression is given by

$$\mathbf{z}_\delta(\theta) = \left[\text{sign}(\theta) \frac{\delta}{\pi} \theta \sin \theta, \frac{\delta}{\pi} \theta \cos \theta \right]^T, \quad (1)$$

where δ is an encoder parameter that determines the distance between the two neighboring spiral arms and θ is the angle from the origin to the point $\mathbf{z} = [z_1, z_2]^T$ on the curve. Notice that the parameter δ determines how the two-dimensional space is filled up and, therefore, how protected the source symbols are against the noise. Hence, the value of δ must be properly selected according to the level of the channel noise or, equivalently, according to the Channel Signal to Noise Ratio (CSNR).

Given a specific spiral defined by its δ value, the compression function $M_\delta(\cdot)$ calculates the value $\hat{\theta}$ corresponding to the point on the spiral that minimizes the distance to \mathbf{x} , i.e.

$$\hat{\theta} = M_\delta(\mathbf{x}) = \underset{\theta}{\text{argmin}} \|\mathbf{x} - \mathbf{z}_\delta(\theta)\|^2. \quad (2)$$

After the analog mapping, a non-linear invertible function $T_\alpha(\hat{\theta}) = \text{sign}(\hat{\theta})|\hat{\theta}|^\alpha$, referred to as the stretching function in [5], is used to produce the encoded symbols \tilde{s} . Although most references in the literature [3–5] use $\alpha = 2$, analog JSCC performance can be significantly improved if α is optimized together with δ [16].

Finally, the encoded symbol \tilde{s} is normalized by $\sqrt{\gamma}$ to ensure the average transmitted power is equal to one. Hence, the symbol sent over the channel is given by

$$s = \frac{T_\alpha(M_\delta(\mathbf{x}))}{\sqrt{\gamma}} = \frac{\tilde{s}}{\sqrt{\gamma}}. \quad (3)$$

When transmitting over an AWGN channel, the received symbols are $y = s + n$ where $n \sim \mathcal{N}(0, N_0/2)$ is a real-valued zero-mean Gaussian random variable that represents the channel noise.

At reception, the analog source symbols are decoded from the observation y . In [17] we proposed a two-stage decoding method that first calculates an estimate of the transmitted channel symbols, \hat{s} , and then performs ML decoding using this symbol estimate. The advantage of such approach is that performance approximates the optimal distortion-cost trade-off in the whole CSNR region while keeping complexity and delay at a minimum [17]. Recently, we have successfully applied this receiver structure to the case of MIMO transmission systems, where the use of the optimal MMSE decoding is clearly infeasible [9, 17]. In Section 3, we will also corroborate that this approach also attains excellent performance in MIMO-OFDM systems.

Analog JSCC can also be used to satisfactorily transmit analog symbols over fading channels. Let us assume a block of T channel symbols s_t , $t = 1, \dots, T$ is transmitted over a Single Input Single Output (SISO) flat fading channel. The block of T received symbols is given by

$$y_t = h_T s_t + n_t, \quad t = 1, \dots, T, \quad (4)$$

where h_T represents the complex-valued channel response and n_t is a block of T zero-mean complex-valued i.i.d. Gaussian random variables that represents the channel noise. We assume a block fading channel whose response remains unchanged during the block transmission. Subindex t denotes discrete-time while subindex T indicates that the channel response changes from one block to another.

In fading channels, the CSNR changes with each channel realization and is given by $\eta_T = |h_T|^2/N_0$. For the considered analog JSCC system to approach the optimal distortion-cost trade-off, the encoder parameters δ and α have to be conveniently optimized. As shown in [17], using $\alpha = 1.3$ provides a good overall performance for a 2:1 compression and a wide range of CSNR and δ values. However, the encoder parameter δ has to be specifically adapted to the CSNR value the channel symbols

will encounter. We have empirically determined, via computer simulations, that using $\alpha = 1.3$ and the two-stage receiver in [17] provides a good overall performance for the case of 2:1 compression in AWGN channels and a wide range of CSNR and δ values. Since choosing $\alpha \neq 2$ makes the analytical optimization of the other encoder parameter, δ , very difficult [4], we obtained the optimum δ values for different CSNRs using off-line computer simulations.

The second row of Table I shows the optimum δ values for the range of CSNR values $0, 1, 2, \dots, 38$ dB and a normalized Gaussian source. In a practical setting, the CSNR can be estimated at the receiver and sent to the transmitter via a limited feedback channel, as shown in Fig. 1. We should also assume that Table I is stored at the transmitter and the receiver for both terminals to determine the correct δ to be used in each transmitted frame.

Another important issue to have in mind is that the normalization factor, γ , corresponds to the mean square value of the symbols at the output of the analog encoder, i.e. $\gamma = \mathbb{E}[|\tilde{s}|^2]$. Due to the non-linear nature of the analog JSCC mappings, the statistical description of \tilde{s} is rather difficult to characterize and strongly depends on the source distribution and the encoder parameter δ . One way to overcome this limitation is to determine off-line, via computer simulations, the mean square value of \tilde{s} for a given source distribution and a set of δ values. The third row of Table I shows the values of γ obtained for the δ values resulting from the encoding optimization for a given CSNR. Note that in fading channels γ has to be continuously adapted, together with δ , according to the CSNR of each specific channel realization. If we assume that the third row of Table I is also stored in the transmitter and the receiver, adaptation of γ is readily done from the CSNR information provided by the feedback channel.

An alternative normalization approach is to determine γ from a channel encoder output block of symbols $\tilde{s}_t, t = 1, \dots, T$. The normalization factor can thus be obtained as

$$\gamma_T = \frac{1}{T} \sum_{t=1}^T |\tilde{s}_t|^2 \quad (5)$$

We will refer to this normalization approach as *deterministic* while the previous one will be termed *statistical*. According to ergodicity, both approaches are related by $\lim_{T \rightarrow \infty} \gamma_T = \gamma$. In practice, however, we have determined via computer simulations that both normalizations provide indistinguishable results for $T > 5$ in both AWGN and Rayleigh fading channels.

The advantage of the deterministic normalization is that it can be calculated online independently of δ . This means that no table of γ values needs to be stored at the transmitter and the receiver, and that the normalization factor can be adapted at a rate different from δ . The drawback is that the receiver needs to know γ_T . However, γ_T is an analog sample that could be sent together with the source symbols. Appending γ_T to the transmitted symbols will cause an overhead of $1/T$ that vanishes as the block size T increases.

3. ANALOG JSCC IN MIMO-OFDM

Figure 2 shows the block diagram of a MIMO-OFDM system that employs analog JSCC. Discrete-time continuous-amplitude symbols are transmitted over a frequency-selective MIMO channel with n_T transmit antennas and n_R receive antennas using an OFDM modulation with K subcarriers.

We extend the analog JSCC design proposed for single-carrier MIMO systems in [9] to the case of multicarrier transmissions over MIMO-OFDM. Thus, source symbols are first spatially multiplexed over the n_T transmit antennas. At each transmit antenna, a set of KN analog source symbols is encoded into K channel symbols using the $N:1$ analog encoding method explained in Section 2. The real-valued symbols at the encoder output are then transformed into complex-valued channel symbols with a complex interleaver. Let $\tilde{S}_{i,k}, i = 1, \dots, n_T, k = 1, \dots, K$, denote the unnormalized encoded symbols transmitted over antenna i and subcarrier k . The corresponding normalized symbols will be represented by $S_{i,k} = \tilde{S}_{i,k} / \sqrt{\gamma_{i,k}}$. In a general setting, both the encoder parameter $\delta_{i,k}$ and the normalization factor $\gamma_{i,k}$ may be different

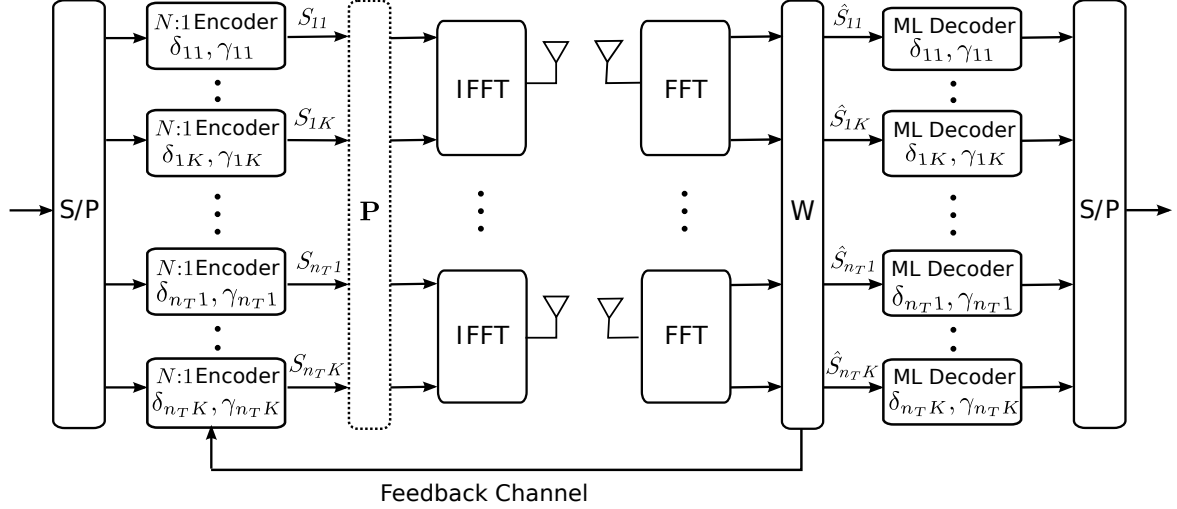


Figure 2. Block diagram of an analog JSCC MIMO-OFDM system.

at each transmit antenna i and/or subcarrier k . Blocks of K normalized channel symbols are put together to be transmitted as OFDM symbols. Let $\mathcal{S}_i = [S_{i,1}, \dots, S_{i,K}]^T$, $i = 1, \dots, n_T$ be the channel symbols that constitute the OFDM symbol transmitted over antenna i . We also define the vector $\mathbf{S}_k = [S_{1,k}, \dots, S_{n_T,k}]^T$, $k = 1, \dots, K$ to represent the MIMO symbols transmitted over subcarrier k .

We assume a block-fading channel that remains unchanged during the transmission of one OFDM symbol. In the time-domain, the block-fading MIMO channel is represented by the sequence of $n_R \times n_T$ matrices $\mathbf{H}[l]$ for $l = 0, \dots, L-1$, where L is the length of the channel impulse response. In a Rayleigh fading MIMO channel, the entries to $\mathbf{H}[l]$ are complex-valued zero-mean circularly-symmetric Gaussian random variables. In the frequency-domain, the MIMO channel response matrices can be expressed as [18]

$$\mathbf{H}_k = \sum_{l=0}^{L-1} \mathbf{R}[l]^{1/2} \mathbf{H}[l] \mathbf{T}[l]^{1/2} \exp\left(\frac{-j2\pi lk}{K}\right), \quad (6)$$

where \mathbf{H}_k is the frequency-domain $n_R \times n_T$ MIMO channel matrix response corresponding to the k -th subcarrier, $k = 1, \dots, K$. Notice that $\mathbf{H}[l]$ entries are i.i.d. random variables whereas $\mathbf{R}[l]$ and $\mathbf{T}[l]$ represent the receive and transmit spatial-correlation matrices, respectively.

In order to eliminate the channel Intersymbol Interference (ISI), an IFFT transformation is applied to the vector of channel symbols \mathcal{S}_i , $i = 1, \dots, n_T$ and a Cyclic Prefix (CP) larger than the channel impulse response is appended at the beginning. These two stages produce the discrete-time representation of the OFDM symbols to be transmitted over the MIMO channel. At reception, the inverse operations of FFT transformation and CP removal are applied. Elaborating the signal model, the received observations \mathbf{Y}_k at subcarrier k are given by

$$\mathbf{Y}_k = \mathbf{H}_k \mathbf{S}_k + \mathbf{N}_k, \quad k = 1, \dots, K \quad (7)$$

where \mathbf{N}_k is an i.i.d. circularly symmetric complex Gaussian random vector that represents the additive spatially and temporally white channel noise.

In analog JSCC, MMSE estimation of the source symbols is the optimal decoding strategy. When considering a MIMO-OFDM system, optimal decoding consists in the calculation, at each subcarrier k , of the MMSE estimate of the Nn_T transmitted source symbols $\mathbf{x}_k = [x_{1,1}, \dots, x_{N,1}, \dots, x_{1,n_T}, \dots, x_{N,n_T}]^T$ from the received symbol vector \mathbf{Y}_k , i.e.

$$\begin{aligned} \hat{\mathbf{x}}_{k,\text{MMSE}} &= \mathbb{E}[\mathbf{x}_k | \mathbf{Y}_k] = \int \mathbf{x}_k p(\mathbf{x}_k | \mathbf{Y}_k) d\mathbf{x}_k \\ &= \frac{1}{p(\mathbf{Y}_k)} \int \mathbf{x}_k p(\mathbf{Y}_k | \mathbf{x}_k) p(\mathbf{x}_k) d\mathbf{x}_k. \end{aligned} \quad (8)$$

where $\mathbb{E}[\cdot]$ denotes the expectation operator. Since the conditional probability, $p(\mathbf{Y}_k|\mathbf{x}_k)$, involves the mapping function $M_\delta(\cdot)$, which is discontinuous and highly non-linear, the integral in (8) can only be calculated numerically. This implies that the discretization of the set of all possible source values, \mathbf{x}_k , is needed. If Q discrete-points are selected per source dimension, we would have to calculate Q^{Nn_T} values for $p(\mathbf{Y}_k|\mathbf{x}_k)$ and $p(\mathbf{x}_k)$, and then compute the integral in (8). This is infeasible in MIMO-OFDM even for a small number of transmit antennas and subcarriers.

Alternatively, the two-stage receiver proposed in [17] for analog JSCC decoding in SISO channels can also be applied to MIMO-OFDM channels. This receiving strategy consists of a first stage where the received symbols are filtered with the aim of minimizing the MSE between the encoder output and the decoder input, and a second step where ML decoding is applied to the filtered symbols to obtain an estimate of the transmitted source symbols.

Assuming \mathbf{H}_k is perfectly known at the receiver, the linear filter \mathbf{W}_k that minimizes the MSE between the channel symbol vector \mathbf{S}_k and the estimated symbol vector $\hat{\mathbf{S}}_k = \mathbf{W}_k \mathbf{y}_k$ is given by

$$\mathbf{W}_k = \left(\mathbf{H}_k^H \mathbf{H}_k + n_T N_0 \mathbf{I}_{n_T} \right)^{-1} \mathbf{H}_k^H, \quad (9)$$

where the super-index H represents conjugate transposition. Then, the set of estimated symbols $\hat{\mathbf{S}}_k = [\hat{S}_{1,k}, \dots, \hat{S}_{n_T,k}]^T$ can be denormalized, transformed into the corresponding real-valued symbols and finally input to a bank of ML decoders to calculate an estimate $\hat{\mathbf{x}}_{i,k}$, $i = 1, \dots, n_T$, of the source symbols transmitted over antenna i and subcarrier k , i.e.

$$\hat{\mathbf{x}}_{i,k} = \mathbf{z}_\delta(\tilde{\theta}_{i,k}) \quad (10)$$

where

$$\tilde{\theta}_{i,k} = T_\alpha^{-1}(\sqrt{\gamma} \hat{S}_{i,k}) = \text{sign}(\hat{S}_{i,k}) |\sqrt{\gamma} \hat{S}_{i,k}|^{-\alpha}. \quad (11)$$

4. ADAPTIVE ANALOG JSCC

As explained in Section 2, optimal encoders have to be used for the analog JSCC system to approximate the optimal distortion-cost trade-off. In the case of MIMO-OFDM systems, the optimization procedure is specially important because symbols transmitted over different antenna i and subcarrier k experience in general a different CSNR, $\eta_{i,k}$. This means that different encoder parameters $\delta_{i,k}$ (and correspondingly, different normalization factors, $\gamma_{i,k}$) should be used when encoding the symbols transmitted over antenna i and subcarrier k .

If no information about the channel is available at the transmitter, the same δ value should be used to encode all the analog source symbols. In this case, it is sensible to use the δ value that corresponds to the average expected CSNR. This fixed approach will perform adequately in frequency-flat and quasi-static channels where the CSNR remains approximately the same at all antennas and all subcarriers during the transmission of several OFDM symbols. However, it can lead to serious performance degradation in practical MIMO-OFDM channels where each subcarrier is expected to have a different time-varying CSNR.

Better performance is obtained when following an adaptive coding strategy where the optimal $\delta_{i,k}$ values are used according to the instantaneous CSNR at each subcarrier and transmit antenna, $\eta_{i,k}$. In a practical setting, this implies that the system be equipped with a feedback channel that regularly sends the $\eta_{i,k}$ values to the transmitter.

In order to appropriately calculate $\eta_{i,k}$, the detector has to be taken into account. When MMSE detection is considered, the filter \mathbf{W}_k does not completely cancel the spatial interference of the MIMO channel. If we consider the residual spatial interference as noise that adds to the thermal noise, it can be shown that the CSNR at the detector output corresponding to the symbols transmitted over the i -th antenna and the k -th subcarrier can

be expressed as [19]

$$\eta_{i,k} = \frac{\mu_{i,k}^2}{\mu_{i,k} - \mu_{i,k}^2} = \frac{\mu_{i,k}}{1 - \mu_{i,k}}, \quad (12)$$

where $\mu_{i,k} = (\mathbf{W}_k \mathbf{H}_k)_{ii}$ is the i -th diagonal entry of the equivalent MIMO channel $\mathbf{W}_k \mathbf{H}_k$.

In summary, the MMSE detector transforms a MIMO-OFDM channel into a set of n_T SISO-OFDM parallel channels, each one with an equivalent CSNR per subcarrier given by (12). At the transmitter, we encode the symbols to be transmitted through each antenna and subcarrier using the appropriate $\delta_{i,k}$ parameter. This parameter is selected from the feedback $\eta_{i,k}$ values and using Table I, which is assumed to be stored at the transmitter and the receiver.

4.1. Analog JSCC MIMO-OFDM with Linear Precoding

If the feedback channel is able to provide the transmitter with the MIMO channel matrices, \mathbf{H}_k , $k = 1, \dots, K$ (and not just the $\eta_{i,k}$ values) further performance improvements can be obtained if channel symbols are precoded prior to their transmission. In digital systems, the water-filling algorithm is the optimal strategy to distribute the transmit power among the streams corresponding to different antennas because it maximizes the channel capacity. However, the performance of analog JSCC systems is commonly measured in terms of the signal distortion. For that reason, following [11], we propose to jointly design a linear precoder and a linear detector suitable for analog JSCC in MIMO-OFDM according to the MMSE criterion.

Recall the MIMO-OFDM signal model defined by (7). Let us assume the output encoder symbols are linearly precoded with a rectangular $n_T \times n_T$ matrix \mathbf{P}_k per subcarrier. Hence the transmitted symbols are $\mathbf{P}_k \mathbf{S}_k$. As in Section 3, \mathbf{W}_k represents the MIMO linear detector per subcarrier. Hence, the channel symbol estimates obtained at the detector output are given by

$$\hat{\mathbf{s}}_k = \mathbf{W}_k (\mathbf{H}_k \mathbf{P}_k \mathbf{S}_k + \mathbf{n}_k), \quad (13)$$

and the error between the estimated and transmitted symbols per subcarrier is

$$\mathbf{e}_k = \mathbf{S}_k - \hat{\mathbf{S}}_k = \mathbf{S}_k - \mathbf{W}_k (\mathbf{H}_k \mathbf{P}_k \mathbf{S}_k + \mathbf{n}_k) \quad (14)$$

The MMSE linear precoder and detector are obtained after solving the following constrained optimization problem

$$\arg \min_{\mathbf{P}_k, \mathbf{W}_k} \sum_{k=1}^K \mathbb{E}[\text{tr}(\mathbf{e}_k \mathbf{e}_k^H)] \quad (15)$$

$$\text{subject to } \sum_{k=1}^K \text{tr}(\mathbf{P}_k \mathbf{P}_k^H) \leq P_{\text{tx}}, \quad (16)$$

where $\text{tr}(\cdot)$ denotes the trace operator and P_{tx} is the total power available at the transmitter.

Substituting the error expression (14) in (15), differentiating with respect to \mathbf{P}_k and \mathbf{W}_k , and using the Karush-Kuhn-Tucker (KKT) conditions, we arrive at the following equations to obtain the optimal \mathbf{P}_k and \mathbf{W}_k matrices

$$\mathbf{P}_k = (\lambda \mathbf{I}_{n_T} + \mathbf{H}_k^H \mathbf{W}_k^H \mathbf{W}_k \mathbf{H}_k)^{-1} (\mathbf{H}_k^H \mathbf{W}_k^H), \quad (17)$$

$$\mathbf{W}_k = (\mathbf{P}_k^H \mathbf{H}_k^H) (n_T N_0 \mathbf{I}_{n_R} + \mathbf{H}_k \mathbf{P}_k \mathbf{P}_k^H \mathbf{H}_k^H)^{-1}, \quad (18)$$

where N_0 is the AWGN noise variance and $\lambda \geq 0$ is the Lagrange multiplier that ensures the total transmit power is equal to P_{tx} . Unfortunately, both equations depend on each other, so we need to iterate between them to calculate the precoder and the detector [11]. The iterative algorithm starts assuming an initial precoder equal to the identity matrix and, at each iteration, both the precoder and the detector are sequentially updated using equations (17) and (18). Notice that the Lagrange multiplier λ is a scalar value that is recalculated at each iteration using Newton's method to ensure that the transmit power constraint is still satisfied. Although the convergence of this algorithm has not been mathematically analyzed, it has been shown to converge after a few iterations in practice for the whole range of CSNRs.

It is important to note that linear precoders change the SNR of the equivalent channel that corresponds to the symbols transmitted over antenna

i and subcarrier k . As a consequence, the encoder parameter $\delta_{i,k}$ should be adapted accordingly. Notice that the CSNR values $\eta_{i,k}$ when linear precoding is used are easy to obtain if we take into account that linear precoders simply transform the MIMO channel \mathbf{H}_k into another one given by $\mathbf{H}_k \mathbf{P}_k$. Hence, the transmitter can calculate the corresponding $\eta_{i,k}$ values using equation (12) and then choosing $\delta_{i,k}$ according to Table I.

4.2. Symbol normalization in MIMO-OFDM

An important issue regarding the optimization of an adaptive analog JSCC MIMO-OFDM system is the normalization of the transmitted symbols $S_{i,k}$. In a non-adaptive system, all subcarriers in the OFDM symbol transmitted over the i -th antenna can be normalized using the same factor γ_i , $i = 1, \dots, n_T$ per antenna. However, when considering adaptive coding, source symbols are encoded with different $\delta_{i,k}$ values that are selected according to the CSNR $\eta_{i,k}$ of the equivalent channel corresponding to antenna i and subcarrier k .

As in Section 2, either a statistical or a deterministic approach can be followed to determine the normalization factors, $\gamma_{i,k}$. In the statistical approach, $\gamma_{i,k}$ should be the mean square value of the unnormalized encoded symbols $\tilde{S}_{i,k}$, i.e. $\gamma_{i,k} = \mathbb{E}[|\tilde{S}_{i,k}|^2]$. For a given source statistics and encoder parameter $\delta_{i,k}$, these mean square values can be estimated off-line via computer simulations and stored in a table such as Table I.

Alternatively, the normalization factors can be obtained following a deterministic approach. Let us assume a block of T OFDM symbols $S_{i,k,t}$, $t = 1, \dots, T$, are transmitted over a block fading channel, i.e.

$$\mathbf{Y}_{k,t} = \mathbf{H}_{k,T} \mathbf{S}_{k,t} + \mathbf{N}_{k,t}, \quad k = 1, \dots, K; \quad t = 1, \dots, T, \quad (19)$$

where the MIMO channel response per subcarrier $\mathbf{H}_{k,T}$ (and hence the equivalent CSNR $\eta_{i,k}$) remains unchanged. The normalization factors can thus be obtained as

$$\gamma_{i,k,T} = \frac{1}{T} \sum_{t=1}^T |\tilde{S}_{i,k,t}|^2 \quad (20)$$

These normalization factors must be known at reception for correct analog decoding. In a practical setup, they can be sent using specific OFDM symbols. This will imply an overhead of $1/T$ that vanishes as the block size T increases.

Contrarily to the single carrier case, the requirement that the channel remains unchanged during the transmission of a block of T OFDM symbols is more difficult to satisfy in practical situations, specially if the FFT size is large. Hence, although the previous deterministic normalization performs well for block sizes as small as $T = 5$, it may be unfeasible in many practical scenarios. This limitation can be overcome by formulating a different deterministic normalization approach where symbols transmitted along subcarriers with similar SNR values are used to estimate their mean square value.

Let us define the set $\mathcal{K}_i = \{1, \dots, K\}$ that contains all subcarriers when transmitting over antenna i . Let us divide the set \mathcal{K}_i into a number of B nonoverlapping subsets $\mathcal{K}_{i,1}, \mathcal{K}_{i,2}, \dots, \mathcal{K}_{i,B}$. The number of elements in these subsets will be represented by $K_{i,1}, K_{i,2}, \dots, K_{i,B}$. Hence, $\mathcal{K}_i = \mathcal{K}_{i,1} \cup \mathcal{K}_{i,2} \cup \dots \cup \mathcal{K}_{i,B}$ and $K_i = K_{i,1} + K_{i,2} + \dots + K_{i,B}$. Recall that in adaptive coding, channel symbols $S_{i,k}$ are obtained with an analog encoder with a parameter $\delta_{i,k}$ that is selected according to the CSNR, $\eta_{i,k}$. Hence, symbols transmitted over subcarriers with similar SNR values will have similar statistics and can be used to estimate their corresponding normalization factor.

Indeed, let us assume that for a given channel realization and a transmit antenna i , the SNRs across the different subcarriers belong to the interval $[\hat{\eta}_{\min}, \hat{\eta}_{\max}]$, i.e. $\hat{\eta}_{\min} \leq \eta_{i,k} \leq \hat{\eta}_{\max}$. Next, we define the subsets $\mathcal{K}_{i,b}$, $b = 1, \dots, B$, as follows:

$$\begin{aligned} \mathcal{K}_{i,1} &= \{k : \hat{\eta}_{\min} \leq \eta_{i,k} < \hat{\eta}_{i,1}\} \\ \mathcal{K}_{i,2} &= \{k : \hat{\eta}_{i,1} \leq \eta_{i,k} < \hat{\eta}_{i,2}\} \\ &\vdots \\ \mathcal{K}_{i,B} &= \{k : \hat{\eta}_{i,B-1} \leq \eta_{i,k} \leq \hat{\eta}_{\max}\} \end{aligned}$$

That is, each subset $\mathcal{K}_{i,b}$, $b = 1, \dots, B$ contains those subcarriers with similar SNR for a given channel realization.

Having in mind the previous subcarrier clustering, we can modify our previous adaptive analog coding approach so that all symbols to be transmitted over the subcarriers in subset $\mathcal{K}_{i,b}$ are encoded with the same representant parameter $\delta_{i,b}$. This is reasonable since all subcarriers in $\mathcal{K}_{i,b}$ have similar CSNR. Hence all channel symbols $S_{i,k}$ with $k \in \mathcal{K}_{i,b}$ have the same statistical properties and their mean square value can be estimated as

$$\gamma_{i,b} = \frac{1}{K_{i,b}} \sum_{k \in \mathcal{K}_{i,b}} |S_{i,k}|^2, \quad i = 1, \dots, n_T, \quad b = 1, \dots, B$$

The choice of the optimal partitioning of the CSNR range into the corresponding B blocks is not trivial because it is necessary to find the set of block limits and representative $\delta_{i,b}$ values that minimize the signal distortion at the receiver. It is not feasible to solve this problem mathematically because the impact of the δ parameter on the overall distortion can be only determined for the case of ML decoding and $\alpha = 2$, as shown [5]. Otherwise, it is rather difficult to characterize the distribution of the coded symbols at the output of the analog encoder and, hence, it not possible to establish a closed-form expression that relates the value of δ and the observed distortion. For that reason, an exhaustive search by computer simulations has been carried out to evaluate the impact of using non-optimal values for δ on the overall distortion and to determine the subcarrier subsets and the representative $\delta_{i,b}$ values of these subsets for different number of blocks. Table II shows the subcarrier subsets and their corresponding representative values $\delta_{i,b}$ obtained for $B = 2, 4$ and 8 assuming that the CSNR values lie within an interval between $\hat{\eta}_{\min} = 0$ dB and $\hat{\eta}_{\max} = 40$ dB.

It is important to note that, similar to other deterministic normalizations, the normalization factors have to be known at reception for the decoders to perform adequately. In a practical setting, the normalization factors can be sent over certain subcarriers within the same OFDM symbols that are specifically reserved to this aim. This will be the approach followed in the sequel. The maximum number of transmitted normalization factors in a limiting situation, where the channel changes at each

OFDM symbol, is B and the maximum overhead that normalization factor transmission implies is B/K . This overhead tends to be negligible as the number of intervals B decreases and/or the FFT size K increases.

In practice, however, the specific number of normalization factors to be transmitted depends on the channel realization and is often less than B . Indeed, in standard MIMO-OFDM channels it is often the case in which subcarrier subsets of a given channel realization are empty and the normalization factor corresponding to this subset need not to be transmitted. This issue is further analyzed in the ensuing section.

4.3. Complexity Analysis

The overall complexity of the analog JSCC MIMO-OFDM system is determined by the filtering operations because the complexity and delay introduced by the analog encoding and ML decoding are practically negligible. On one hand, the analog encoding consists in mapping the bidimensional point given by two source symbols into the closest point on the spiral and applying the stretching function to the corresponding angle from the origin to that point. Efficient search algorithms can be employed to determine the closest point on the spiral with low complexity. On the other hand, the ML decoding basically inverts the encoding operations and the complexity is hence identical.

The overall complexity depends on the transmission strategy considered in the analog JSCC MIMO-OFDM system. In the case of non-adaptive and adaptive coding, a linear MMSE detector is used for filtering the received symbols. The complexity of such filtering operation is $\mathcal{O}(n_T^3)$ because it involves several products of matrices and especially the inverse of an $n_T \times n_T$ -sized matrix. Notice that the complexity of both transmission strategies is the same since the main difference of the adaptive coding with respect to the non-adaptive method is the use of information about the estimated SNR to select the optimal encoder parameters at the transmitter.

In the case of the adaptive coding with linear precoding, the optimal linear MMSE filters for each subcarrier are individually calculated by an iterative

algorithm that sequentially updates the precoder and the corresponding detector. On one hand, the algorithm complexity at each iteration is $\mathcal{O}(M^3)$, where $M = \max\{n_T, n_R\}$, because the expressions for the transmit and receive filters also involve the inverse of an matrix of size $n_R \times n_R$ and $n_T \times n_T$, respectively. On the other hand, the number of iterations required for the iterative algorithm to converge basically depends on the CSNR. In the high CSNR region, it can be shown that the MSE cost function is almost flat and, thus, a large number of iterations is required to converge whereas for low CSNRs the algorithm converges after very few iterations. In practice, the computation of the optimal MMSE filters never exceeds 50 iterations. Notice that these filters are obtained once for each channel realization and must only be recalculated when the channel changes.

5. SIMULATION RESULTS

Computer simulations were carried out to assess the performance of the analog JSCC MIMO-OFDM systems considered in previous sections. Three different configurations were evaluated: non-adaptive coding, adaptive coding and adaptive coding with linear precoding.

System performance is measured in terms of the Signal to Distortion Ratio (SDR) with respect to the average CSNR. If the MSE between decoded and source analog symbols, i.e.

$$\text{MSE} = \frac{1}{N} \mathbb{E}\{\|\mathbf{x} - \hat{\mathbf{x}}\|^2\},$$

is selected as the distortion metric, the SDR in dB can be calculated as

$$\text{SDR}_{(dB)} = 10 \log_{10} \left(\frac{\sigma_x^2}{\text{MSE}} \right), \quad (21)$$

where σ_x^2 is the source variance. The optimal distortion-cost trade-off is the maximum attainable SDR for a given CSNR. In the literature, this theoretical limit is known as the Optimum Performance Theoretically Attainable (OPTA) and is calculated by equating the rate distortion function

to the channel capacity [20]. For $N:1$ compression of Gaussian sources over a generic stochastic $n_R \times n_T$ channel matrix \mathbf{H}_k , and assuming that the channel is not known at the transmitter, the OPTA is given by

$$N n_T \log(\text{SDR}) = \mathbb{E}_{\mathbf{H}_k} \left[\log \det \left(\mathbf{I}_{n_R} + \frac{\eta}{n_T} \mathbf{H}_k \mathbf{H}_k^H \right) \right], \quad (22)$$

where $\mathbb{E}_{\mathbf{H}_k}[\cdot]$ represents expectation with respect to \mathbf{H}_k and η is the average CSNR. In a system where the channel is known at the transmitter, capacity is maximized by the water-filling solution at each channel realization. In our case, however, channel knowledge at transmission is not exploited to maximize capacity but to precode transmitted symbols with the linear MMSE precoding matrices \mathbf{P}_k , $k = 1, \dots, K$, given by (17). Therefore, OPTA is calculated in this case by replacing \mathbf{H}_k with the equivalent channel $\mathbf{H}_k \mathbf{P}_k$ in (22).

Let us start by considering the case $n_T = n_R = 1$, i.e. SISO-OFDM. We considered a source of i.i.d. normalized Gaussian random variables and $K = 64$ subcarriers. In a first computer experiment we considered real wireless channels measured in an indoor scenario (an office) by using a hardware testbed which was jointly designed and implemented by two research groups from the Universities of Cantabria (UC) and A Coruña (UDC) in Spain for the practical evaluation of multiuser multiantenna transmission techniques. This testbed consists of three transmit and three receive nodes each equipped with MIMO capabilities. For a detailed description of the GTEC MIMO testbed, see the URL of the COMONSENS project [21].

In this first experiment, the real channel measurements were specifically obtained for 64 subcarriers using one single transmit antenna and one single receive antenna, which are at a distance of approximately 9 m with direct line-of-sight. Figure 3 plots the Power Delay Profile (PDP) of such measured indoor channels. The corresponding RMS delay spread is 6 nanoseconds. In addition, it has been observed that the channel frequency response values at each subcarrier approximately follow a Rayleigh distribution although with a different variance at each subcarrier.

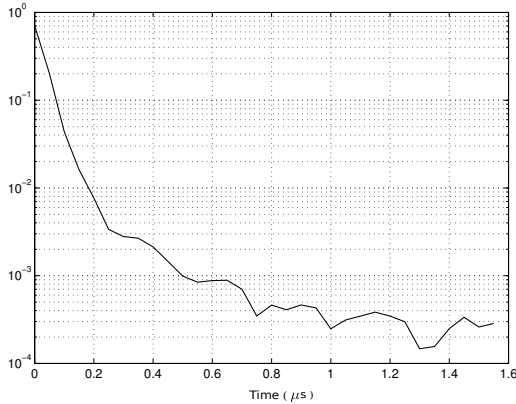


Figure 3. Power delay profile of the measured real indoor channel

Figure 4 plots the obtained results. It can be seen that the three proposed analog JSCC techniques approach the OPTA in the whole SNR region. As expected, the worst performance is obtained when no CSI is available at the transmitter (i.e. non-adaptive coding and no precoding), specially when the CSNR is high in which case performance is almost 4.0 dB below the OPTA. Performance is significantly improved (about 1.8 dB at high SNR) when adaptive coding is considered and further improvement can be obtained if MMSE linear precoding is utilized. This latter improvement, however, is relatively small because we are in a SISO scenario and not much performance gain should be expected from linear precoding. Stochastic normalization was used in the adaptive coding approaches, but the same results were obtained with per-subcarrier deterministic normalization and $B = 8$ blocks.

In a second computer experiment for SISO-OFDM, we considered the ITU-Pedestrian B model. For a complete description of the delay and Doppler power profiles of such model see reference [22]. Doppler shift is assumed low enough so that the channel remains unchanged during the transmission of an OFDM symbol and no Inter Carrier Interference (ICI) arises. In the ITU-Pedestrian B channel model this condition is met for a reasonable large number of practical situations. Nevertheless, the channel changes from one OFDM symbol to another according to the Doppler power profile of the model. In the adaptive coding

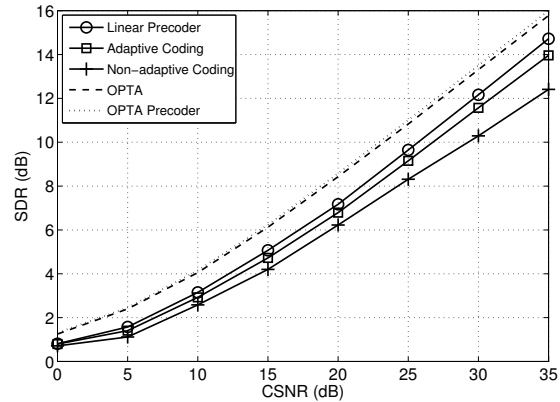


Figure 4. Performance of 2:1 analog JSCC SISO-OFDM systems over measured real channels.

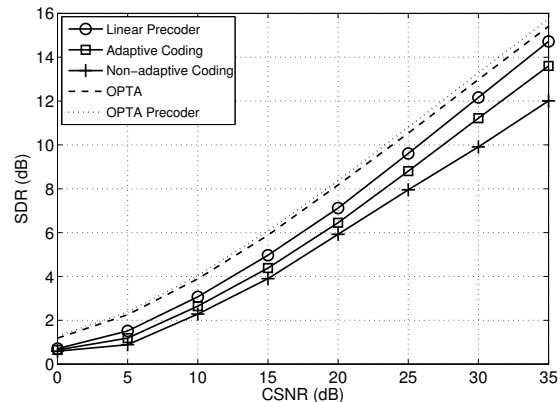


Figure 5. Performance of 2:1 analog JSCC SISO-OFDM systems over a Pedestrian B model.

approaches, the encoder parameters are adjusted at each OFDM symbol and stochastic normalization was used. Figure 5 shows the obtained results which are similar to those presented in Figure 4, although the performance gains when considering adaptive coding and linear precoding are slightly higher.

We now shift our focus to MIMO-OFDM channels. Let us start by considering real 4×4 MIMO-OFDM fading channels measured using the GTEC MIMO testbed described above in the same indoor scenario and for $K = 64$. Stochastic normalization was used in the adaptive coding approaches, but the same results were again obtained with per-subcarrier deterministic normalization and $B = 8$ blocks. Figure 6 plots the obtained results. The non-adaptive coding strategy exhibits the worst performance. It is 8.0 dB below the OPTA at high

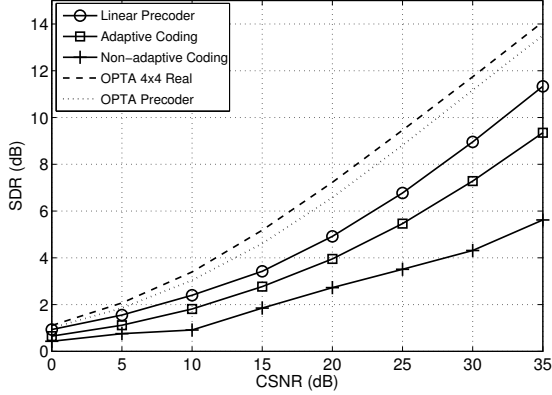


Figure 6. Performance of analog JSCC 4×4 MIMO-OFDM systems over measured real channels.

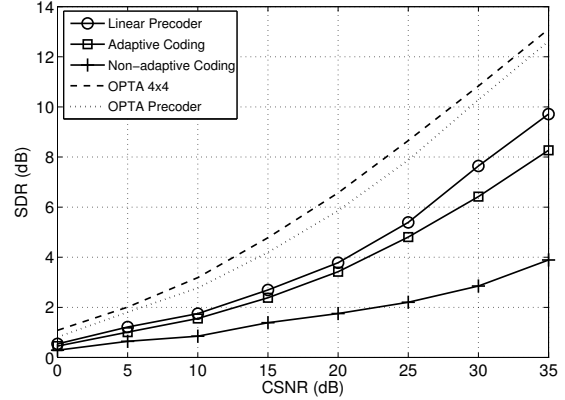


Figure 7. Performance of analog JSCC 4×4 MIMO-OFDM systems over an IMETRA-D channel.

channel SNR values. A significant improvement in performance is obtained (3.5 dB at high SNR) when considering adaptive coding. Different to the SISO case, performance also improves significantly (2 dB at high SNR) when incorporating linear MMSE precoding. It is interesting to note from Figure 6 that the OPTA with precoding is actually lower than that without precoding. This is because the precoder has been designed to minimize the MSE and not to maximize capacity. Nevertheless, notice that the actual performance of the precoded system is better than that of the system without precoding.

We also carried out computer experiments considering a standard model such as the Intelligent Multi-element Transmit and Receive Antennas case D (IMETRA-D) channel model described in [23]. The IMETRA-D model only specifies the spatial correlation of a MIMO channel, i.e. the matrices $\mathbf{R}[l]$ and $\mathbf{T}[l]$ in (6). For the delay and Doppler power profile we chose the same parameters as in the ITU-pedestrian B model [22]. Figure 7 plots the obtained results which highlight the importance of the adaptive coding strategies. Indeed, without adapting the analog encoder parameters, system performance is very far away from the OPTA (9.5 dB at high SNR). With adaptive coding the gap to the OPTA reduces significantly (5.0 dB at high SNR) while the distance to the OPTA is even less (less than 3 dB at high SNR) when adaptive coding with linear precoding is utilized.

It is important to note that the deterministic normalization based on temporal averaging cannot be used when transmitting over this type of time varying channels. In such cases, the subcarrier clustering deterministic normalization described in Section 4.2 should be used. Figure 8 plots the performance of an analog JSCC 4×4 MIMO-OFDM system with adaptive coding and precoding when transmitting over an IMETRA-D channel for different values of B , i.e. the number of subsets in which we divided the CSNR range $[\hat{\eta}_{\min}, \hat{\eta}_{\max}]$. Similar behavior as a function of B was observed for the case of adaptive coding without precoding. The subset limits and the encoder representant values $\delta_{i,b}$ are those in Table II. Figure 8 also plots the limiting case $B = 40$ in which there is a subset per CSNR integer value in dB (see Table I). The results shown in Figure 8 indicate that the SDR decreases very slightly when $B \geq 4$ (less than 0.5 dB) with respect to the per-SNR normalization. Performance starts degrading significantly when B is less than 4.

As explained before, deterministic normalization has the inconvenience that the normalization factors have to be transmitted, hence increasing the system overhead. Nevertheless, the fact that the number of subcarrier subsets can be significantly reduced without degrading performance enables the system to reduce the number of normalization factors to be transmitted. Figure 9 illustrates this issue by plotting the overhead percentage for different

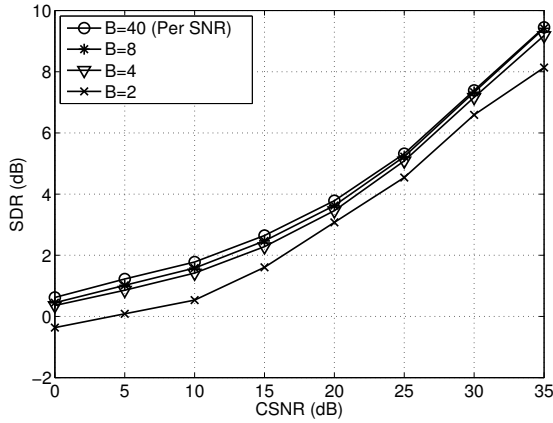


Figure 8. Performance with respect to B of an analog JSCC 4×4 MIMO-OFDM system with deterministic normalization over an IMETRA-D channel.

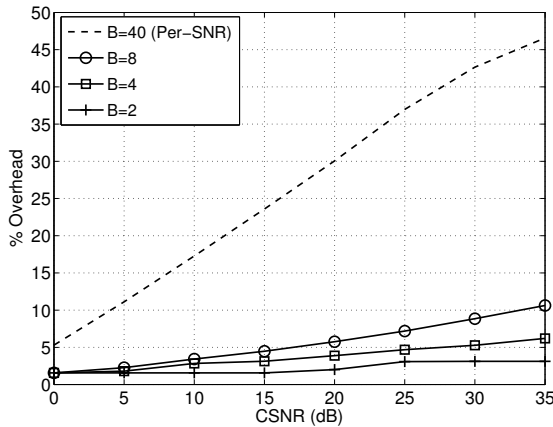


Figure 9. Overhead caused by deterministic normalization in an analog JSCC 4×4 MIMO-OFDM system over an IMETRA-D channel.

values of CSNR and B . Notice that the per-SNR normalization ($B = 40$) demands a significant overhead, which can be as high as 50 % at high CSNR values. At lower SNRs the overhead is less because the number of empty SNR subsets increases and it is not necessary to send their normalization factors. As shown in Figure 9, overhead reduces significantly for $B = 2, 4$ and 8.

In summary, according to Figures 8 and 9 the choice $B = 4$ attains a good trade-off between performance and overhead. The number of normalization factors to be sent can be greatly reduced, with a negligible impact on performance, from almost 50% to just 6% in the worst case.

6. CONCLUSIONS

We have studied the analog transmission of discrete-time coded samples using a MIMO-OFDM system. Source symbols are analog JSCC encoded and sent as OFDM symbols over frequency-selective MIMO fading channels. As an alternative to optimal MMSE decoding, we proposed a more practical two-stage receiver made up of a MMSE estimator followed by a Maximum Likelihood (ML) decoder. This approach exhibits a satisfactory performance in the whole SNR region while keeping complexity and delay at a minimum. We studied three different alternatives for system optimization: non-adaptive coding, adaptive coding and adaptive coding with precoding. Simulation results show that the three analog JSCC transmission strategies approach the optimal distortion-cost trade-off (i.e. the OPTA), and the best performance is obtained when using the adaptive coding together with precoding. We have also paid special attention to the normalization of the analog encoded symbols. A deterministic normalization approach has been proposed that can be applied to each OFDM symbol individually, while significantly reducing the overhead caused by the transmission of the normalization factors.

7. ACKNOWLEDGEMENTS

This work has been funded by Xunta de Galicia, Ministerio de Economía y Competitividad of Spain, and FEDER funds of the European Union under grants 2012/287, TEC2010-19545-C04-01, and CSD2008-00010. This research has been also supported by the Air Force Research Laboratory under agreement number FA9550-12-1-0086. The U.S. Government is authorized to reproduce and distribute reprints for Governmental purposes notwithstanding any copyright notation thereon. The views and conclusions contained herein are those of the authors and should not be interpreted as necessarily representing the official policies or endorsements, either expressed or implied, of the Air Force Research Laboratory or the U.S. Government.

REFERENCES

1. Shannon CE. A mathematical theory of communication. *The Bell System Technical Journal* 1948; **7**:379–423.
2. Berger T. *Rate Distortion Theory: A Mathematical Basis for Data Compression*. Englewood Cliffs, 1971.
3. Chung SY. On the construction of some capacity-approaching coding schemes. *Ph.D. Dissertation, Dept. EECS, MIT* 2000; .
4. Ramstad TA. Shannon mappings for robust communication. *Teletronikk* 2002; **98**(1):114–128.
5. Hekland F, Floor P, Ramstad TA. Shannon-Kotel'nikov mappings in joint source-channel coding. *IEEE Trans. on Communications* Jan 2009; **57**(1):94–105.
6. Kansanen K, Kim A, Thobaben R, Karlsson J. Low complexity bandwidth compression mappings sensor networks. *Proc. Int. Symposium on Communications, Control, and Signal Process. (ISCCSP)*, 2010.
7. de Oliveira Brante G, Souza R, Garcia-Frias J. Analog joint source-channel coding in Rayleigh fading channels. *Proc. IEEE Int. Conf. Acoustics, Speech, Signal Process. (ICASSP)*, 2011; 3148–3151.
8. Brante G, Souza R, Garcia-Frias J. Spatial diversity using analog joint source channel coding in wireless channels. *IEEE Trans. on Communications* 2013; **61**(1):301–311.
9. Vazquez-Araujo F, Fresnedo O, Castedo L, Garcia-Frias J. Analog joint source-channel coding over MIMO channels. *EURASIP Journal on Wireless Communications and Networking* 2014; **2014**:25(1), doi:10.1186/1687-1499-2014-25.
10. Garcia-Naya JA, Fresnedo O, Vazquez-Araujo FJ, Gonzalez-Lopez M, Castedo L, Garcia-Frias J. Experimental evaluation of analog joint source-channel coding in indoor environments. *Proc. IEEE International Conference on Communications (ICC)*, 2011.
11. Sampath H, Stoica P, Paulraj A. Generalized linear precoder and decoder desing for MIMO channels using the weighted MMSE criterion. *IEEE Trans. on Communications* Dec 2008; **49**(12):2198–2206.
12. Scaglione A, Giannakis G, Barbarossa S. Redundant filterbank precoders and equalizers. i. unification and optimal designs. *IEEE Transactions on Signal Processing* Jul 1999; **47**(7):1988 – 2006.
13. Kejalakshmi V, Arivazhagan S. Design of linear precoder for multiuser MIMO system with spatial correlation and imperfect CSI. *Trans. on Emerging Telecommunications Technologies* Nov 2013; .
14. Hekland F, Oien GE, Ramstad TA. Using 2:1 Shannon mapping for joint source-channel coding. *Proc. Data Compression Conference (DCC)*, 2005.
15. Akyol E, Rose K, Ramstad T. Optimal mappings for joint source channel coding. *Proc. Information Theory Workshop (ITW)*, 2010.
16. Hu Y, Garcia-Frias J, Lamarca M. Analog joint source-channel coding using non-linear curves and MMSE decoding. *IEEE Trans. on Communications* Nov 2011; **59**(11):3016–3026.
17. Fresnedo O, Vazquez-Araujo F, Castedo L, Garcia-Frias J. Low-complexity near-optimal decoding for analog joint source channel coding using space-filling curves. *IEEE Communications Letters* Apr 2013; **17**(4):745–748.
18. Lu B, Yue G, Wang X. Performance analysis and design optimization of LDPC-coded MIMO OFDM systems. *IEEE Trans. on Signal Processing* Feb 2004; **52**(2):348–361.
19. Wang X, Poor HV. Iterative (turbo) soft interference cancellation and decoding for coded CDMA. *IEEE Trans. on Communications* jul 1999; **47**(7):1046–1061.
20. Berger T, Tufts D. Optimum pulse amplitude modulation–I: transmitter-receiver design and bounds from information theory. *IEEE Trans. on Information Theory* Apr 1967; **13**(2):196 – 208.
21. COMONSENS project. <http://www.comonsens.org/>.
22. ITU ITU-R M1225. Guidelines for evaluation of radio transmission technologies for IMT-2000. <http://www.itu.int/rec/R-REC-M.1225/en>

1997.
23. IST-METRA project. <http://www.ist-metra.org>.

CSNR (dB)	0	1	2	3	4	5	6	7	8	9	10	11	12
δ	9.8	8.0	5.6	5.0	4.2	4.0	3.9	3.7	3.6	3.4	3.2	3.1	3.0
γ	0.1	0.11	0.12	0.14	0.16	0.2	0.6	1.2	1.9	2.5	3.0	3.3	3.5
CSNR (dB)	13	14	15	16	17	18	19	20	21	22	23	24	25
δ	2.9	2.7	2.5	2.3	2.2	2.1	2.0	1.8	1.7	1.5	1.4	1.3	1.2
γ	3.9	4.7	5.7	7.1	7.9	8,9	10.0	13.1	15.1	20.5	24.5	29.7	35.3
CSNR (dB)	26	27	28	29	30	31	32	33	34	35	36	37	38
δ	1.1	1.0	0.9	0.8	0.8	0.8	0.7	0.7	0.6	0.6	0.5	0.5	0.4
γ	45	56	74	99	99	99	140	140	209	209	333	333	588

Table I. Optimal values for δ and γ for 2:1 analog JSCC and Gaussian sources.

Number of intervals	CSNR range (dB)	$\delta_{i,b}$ values
$B = 2$	[0-20]	2.3
	[21-40]	0.8
$B = 4$	[0-8]	8.0
	[9-19]	2.2
	[20-29]	0.9
	[30-40]	0.5
$B = 8$	[0-7]	8.0
	[8-14]	3.0
	[15-20]	2.0
	[21-25]	1.3
	[26-30]	0.8
	[31-34]	0.7
	[25-37]	0.5
[38-40]	0.4	

Table II. Subcarrier partitioning for deterministic normalization